Bayesian-Based Ensemble Source Apportionment of PM$_{2.5}$

Sivaraman Balachandran,*,[†] Howard H. Chang,[‡] Jorge E. Pachon,[§] Heather A. Holmes,[†] James A. Mulholland,[†] and Armistead G. Russell[†]
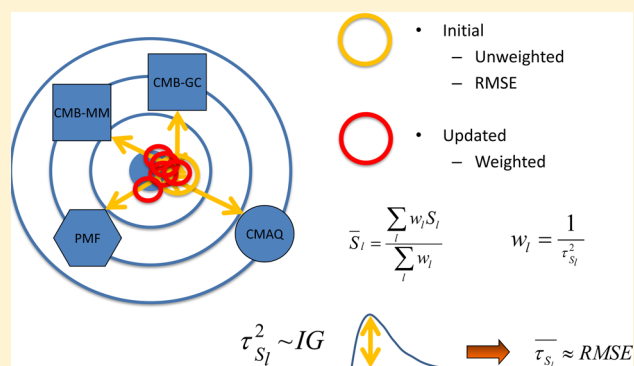
[†]School of Civil and Environmental Engineering, Georgia Institute of Technology, Atlanta, Georgia 30332, United States
[‡]Rollins School of Public Health, Emory University, Atlanta, Georgia 30322, United States
[§]Programa de Ingenieria Ambiental, Universidad de La Salle, Bogota, Colombia

Ⓢ *Supporting Information*

ABSTRACT: A Bayesian source apportionment (SA) method is developed to provide source impact estimates and associated uncertainties. Bayesian-based ensemble averaging of multiple models provides new source profiles for use in a chemical mass balance (CMB) SA of fine particulate matter (PM$_{2.5}$). The approach estimates source impacts and their uncertainties by using a short-term application of four individual SA methods: three receptor-based models and one chemical transport model. The method is used to estimate two seasonal distributions of source profiles that are used in SA for a long-term PM$_{2.5}$ data set. For each day in a long-term PM$_{2.5}$ data set, 10 source profiles are sampled from these distributions and used in a CMB application, resulting in 10 SA results for each day. This formulation results in a distribution of daily source impacts rather than a single value. The average and standard deviation of the distribution are used as the final estimate of source impact and a measure of uncertainty, respectively. The Bayesian-based source impacts for biomass burning correlate better with observed levoglucosan ($R^2 = 0.66$) and water-soluble potassium ($R^2 = 0.63$) than source impacts estimated using more traditional methods and more closely agrees with observed total mass. The Bayesian approach also captures the expected seasonal variation of biomass burning and secondary impacts and results in fewer days with sources having zero impact. Sensitivity analysis found that using non-informative prior weighting performed better than using weighting based on method-derived uncertainties. This approach can be applied to long-term data sets from speciation network sites of the United States Environmental Protection Agency (U.S. EPA). In addition to providing results that are more consistent with independent observations and known emission sources being present, the distributions of source impacts can be used in epidemiologic analyses to estimate uncertainties associated with the SA results.

INTRODUCTION

Air quality standards are driven, in part, by health impacts of air pollutants, and the policies to control sources of air pollutants are often evaluated by improvements to human health. Ambient air pollution has been estimated to contribute to greater than 3 000 000 premature deaths worldwide in 2010; of this burden, the vast majority has been attributed to fine particulate matter (PM$_{2.5}$).[1] PM$_{2.5}$ health impacts include both respiratory and cardiovascular health outcomes.[2,3] Given the potential health impacts, the United States Environmental Protection Agency (U.S. EPA) has set National Ambient Air Quality Standards (NAAQS) for PM$_{2.5}$, and a major goal for states and regional communities is to meet those standards and protect public health. It is suspected that PM$_{2.5}$ health effects vary by composition and source and may depend upon the mixture of pollutants, leading to efforts to estimate relationships between sources of PM$_{2.5}$ and health effects.[4−8]

Controlling ambient PM$_{2.5}$ concentrations ultimately means controlling sources of PM$_{2.5}$, which requires techniques for estimating source contributions. However, PM$_{2.5}$ sources typically emit a mixture of pollutants, including gases and particles, which mix in the atmosphere and can undergo chemical transformations prior to impacting a specific receptor location, making it difficult to quantify impacts. Source apportionment (SA) involves one or more techniques that are used to quantify how individual sources contribute to PM$_{2.5}$ concentrations. SA techniques that rely on statistical analysis of observations at monitor sites are referred to as receptor models. These techniques include chemical mass balance (CMB) and positive matrix factorization (PMF). In addition, chemical transport models (CTMs) have used sensitivity parameters to estimate source contributions. These different SA approaches often result in source contributions that can differ in magnitude and/or are poorly correlated (see Table S1 of the Supporting Information). Determining which method's set of source

contributions is the most accurate is further complicated because source impacts, in general, cannot be directly measured. Without direct measurement of source impacts, methods for estimating uncertainty vary across the SA approaches, making it difficult to directly compare uncertainties across methods. For example, some methods (e.g., CTMs) have not provided source impact estimate uncertainties, while others use bootstrapping or propagation of errors to estimate uncertainties.

In this work, we build on an approach to combine multiple SA model results to train a CMB method for long-term application[9−11] by extending the ensemble technique to include a Bayesian formulation of weights used in ensemble-averaging source impacts. In a Bayesian approach, probabilistic distributions of the parameters of interest are estimated using prior distributions, along with information from observed data. Bayesian analysis has been used in a variety of applications and can be especially useful for estimating model parameters that are weakly informed by the observed data.

Bayesian techniques have previously been used in SA of $PM_{2.5}$[12−18] to estimate the model parameter, including source impacts, which are positive and lognormally distributed. In this work, a method is developed that incorporates Bayesian techniques to estimate SA uncertainties. These uncertainties are then used as weights to estimate an ensemble average of source impacts similar to work by Lee et al.[10] and Balachandran et al.[9] The Bayesian framework for estimating SA uncertainties requires first placing prior distributions about a subjective (expert-driven) view of uncertainties associated with each SA method. Next, the root-mean-square error (RMSE) between an initial ensemble average and each individual method is used as the updated information about source impact uncertainties. Using an inverse gamma (IG) prior to a normal data likelihood leads to an IG posterior distribution of uncertainties for each SA method. These uncertainty distributions are then used as weights to obtain an updated ensemble. One advantage of this method is that it obviates the need to assume lognormally distributed data sets. This assumption can be problematic for receptor models, which can result in zero or negative impacts. Also, the approach incorporates several different models and provides a way to compare methods using a consistent estimation of uncertainties.

The objective of this work is to refine our previously developed ensemble approach for apportioning $PM_{2.5}$ to sources by incorporating a Bayesian technique to obtain multiple realizations of ensemble-averaged source impacts, which are subsequently used for deriving multiple realizations of source profiles. We then compare results using this approach to results using our previous ensemble approach as well as results using individual receptor models.

■ METHODS

Ensemble Averaging. The method developed here extends an ensemble SA method[10,9] and comprises three steps: (1) Bayesian ensemble-averaging source impacts over a short-term time period, (2) using these source impacts to develop regionally and seasonal specific source profiles, and (3) using the new source profiles to apportion sources for a long-term data set. We use SA results from three receptor models and one chemical transport model for July 2001 and January 2002. We use two CMB methods: CMB-LGO,[19] which incorporates gas-based constraints, and CMB-MM,[20] which uses molecular marker observations. We use one factor analytic

method, PMF[21] and one CTM, the community multiscale air quality (CMAQ) model.[22] We use results from previous work for CMB-MM[23] and CMAQ with tracers.[24] We also applied EPA-CMB, version 8.0 (referred to here as CMB-RG, for "regular"),[25,26] but these results were used for comparison and were not included in the ensemble.

In the work developed by Balachandran et al.,[9] an ensemble average of source impacts is calculated in a two-step process. First, an equally weighted average of source impacts is calculated (eq 1, with $N = 0$ in eq 2)

$$\overline{S}_{jk} = \frac{\sum_{l=1}^{L} w_{jlk} S_{jlk}}{\sum_{l=1}^{L} w_{jlk}} \tag{1}$$

$$w_{jlk} = \frac{1}{\tau_{S_{ljk}}^{N}} \tag{2}$$

where w_{jlk} is the weight for source j from method l on day k and S_{jlk} is the source impact for source j from method l on day k. Next, the root-mean-square error (RMSE) is calculated between each method and the ensemble average (eq 3).

$$RMSE_{jl} = \sqrt{\frac{\sum_{k=1}^{K} (S_{jlk} - \overline{S}_{jk})^2}{K}} \tag{3}$$

The uncertainty is set to be equal to the RMSE of each method, and the square is used to weight an updated ensemble average (eq 2, with $N = 2$ and τ = RMSE). Finally, the uncertainty of the updated ensemble average is calculated using weighted propagation of errors with covariance.[9] To compare the ensemble to the individual SA methods, we use the root-mean-square average of the daily source impact uncertainties to reflect the overall method uncertainty $(\overline{\sigma}_{S_{jlk}})$[9,27] (eq 4).

$$\overline{\sigma}_{S_{jl}} = \sqrt{\frac{1}{K} \sum_{k=1}^{K} \sigma_{S_{jlk}}^2} \tag{4}$$

Bayesian Ensemble Averaging. One limitation of the method described above is that, for any source (for any method), the estimated source impact uncertainty is the same for each day, because the RMSE does not change on a daily basis. A more realistic interpretation is that the RMSE should be viewed as an "average" uncertainty and that the true uncertainty comes from a distribution whose mean is equal to the RMSE. In Bayesian ensemble averaging, a posterior distribution of uncertainties is calculated using a prior distribution and treating the estimated RMSEs as the data. For each day of the short-term application of the four SA methods, source impact uncertainties are sampled from the Bayesian-based posterior distribution using a Monte Carlo technique. These uncertainties are used as weights to calculate ensemble-averaged source impacts.

It is assumed that estimates of source impacts vary randomly around "true" source impacts (see the Supporting Information for further discussion of potential biases). Therefore, S_{jlk}, the impact from source j and method l on day k, can be viewed as a surrogate measure of the true source impact and that the average of these methods, $\overline{S}_{jk}$, can be treated as the true source impact. A consequence is that that these errors are normally distributed, so that for any day k

$$S_{jlk} - \overline{S}_{jk} \sim \text{normal}(0, \tau_{jlk}^2) \tag{5}$$

We wish to obtain posterior samples of τ_{jlk}^2 and use them to calculate an ensemble average using eqs 1 and 2. First, we assign an IG (scaled inverse χ^2) distribution to each variance component. The IG distribution is specified by a density function with two known parameters α and β and denoted as IG(α, β).

$$f(\tau_{jlk}^2 | \alpha, \beta) = \frac{\beta^\alpha}{\Gamma(\alpha)} (\tau_{jlk}^2)^{-\alpha-1} \exp\left(-\frac{\beta}{\tau_{jlk}^2}\right) \quad (6)$$

The error of the data $[S_{jl}(k=1), ..., S_{jl}(k=K)]$ with respect to the average has a likelihood given by the normal density.

$$f(\text{data} | \tau_{jlk}^2) = (2\pi\tau_{jlk}^2)^{-K/2} \exp\left(-\frac{1}{2\tau_{jlk}^2} \sum_{k=1}^{K} (S_{jlk} - \bar{S}_{jk})^2\right) \quad (7)$$

The posterior distribution of τ_{jlk}^2 given the data is found from

$$f(\tau_{jlk}^2 | \text{data}) \propto f(\text{data} | \tau_{jlk}^2) f(\tau_{jlk}^2 | \alpha, \beta) = (\tau_{jlk}^2)^{-(\alpha + \frac{K}{2}) - 1}$$
$$\exp\left(-\frac{1}{\tau_{jlk}^2}\left[\beta + \frac{1}{2}\sum_{k=1}^{K}(S_{jlk} - \bar{S}_{jk})^2\right]\right) \quad (8)$$

The last expression is proportional to an IG distribution.

$$\text{IG}\left(\alpha + \frac{K}{2}\left[\beta + \frac{1}{2}\sum_{k=1}^{K}(S_{jlk} - \bar{S}_{jk})^2\right]\right) \quad (9)$$

It is important to note that the above distribution has mean

$$\frac{\left[\beta + \frac{1}{2}\sum_{k=1}^{K}(S_{jlk} - \bar{S}_{jk})^2\right]}{\alpha + \frac{K}{2}} \quad (10)$$

and for small values of α and β, the mean is approximately the square of the RMSE in eq 3. Typically, prior information about τ_{jlk}^2 can be incorporated in α and β. We approach this method in two ways. To reflect a lack of knowledge, we can use non-informative priors by setting $\alpha = \beta = 0.0001$. In addition, we can use the distribution of method-specific uncertainties and have informative priors (see Figure S1 of the Supporting Information). For CMAQ, we use non-informative prior information because uncertainties are not directly available from the model application. Again, this allows us to sample multiple realizations of weights (i.e., uncertainties) that are used in ensemble averaging. Ensemble averaging is conducted for 30 days in the summer (July 2001) and 30 days in the winter (January 2002). For each day in the ensemble, we used 30 samples from the posterior distributions, resulting in 30 ensemble-averaged source impact estimates for each of the 30 days in the short-term period.

Development of Seasonal Source Profiles. We develop source profiles in the same manner as Lee et al.[10] We solve the chemical mass balance equation (eq 11), where C_i is the measured concentration of species i, and treat the source profile matrix, f_{ij}, as the unknown and the source contribution, S_j, as known using the ensemble-based source impacts ($\bar{S}_j$).

$$C_i = f_{ij}\bar{S}_j + e_i \quad (11)$$

The source profiles, f_{ij}, are recalculated using a nonlinear optimization program (the Lipschitz Global Optimizer) to minimize the χ^2 value

$$\chi_k^2 = \sum_{i=1}^{I} \frac{(C_{ik} - \sum_{j=1}^{J} f_{ij}\bar{S}_j)^2}{\sigma_{C_{ik}}^2} \quad (12)$$

where $\sigma_{C_{ik}}^2$ is the square of the measurement uncertainty of species i on day k. Source profiles, f_{ij}, are estimated simultaneously, for each day, for the primary sources GV, DV, DUST, BURN, and COAL. The optimization is constrained to ensure that estimates of new source profiles are realistic. These constraints include that the sum of PM$_{2.5}$ species in the source profiles, accounting for mass from metal oxides and organic matter, is less than 1. There are also lower and upper bounds for all species in the derived source profiles. These bounds are set to be between $1/3$ and 3 times the average values in measurement-based source profiles (MBSPs).[19] When 3 times the average for a specific species is greater than 1, the upper bound is set to 0.99.

This optimization is conducted for each set of ensemble-averaged source impacts. For the standard ensemble, we use ensemble-averaged source impacts from Balachandran et al.[9] to calculate ensemble-based source profiles (EBSPs) for 30 days in July 2001 (summer) and January 2002 (winter) each. For the Bayesian ensemble, source profiles are derived for both the non-informative prior and informative prior cases. We sample 30 estimates of weights for each of the 30 days in the ensemble; this leads to 900 source profiles for summer and winter each, which represent distributions of two seasonal Bayesian ensemble-based source profiles (BBSPs). For the EBSPs, the average of the 30 source profiles is used in the long-term SA and the standard deviation is treated as the source profile uncertainty. For the Bayesian ensemble, profiles used in the SA are sampled from the distribution of 900 source profiles. Because we have 30 replicates of 30 days in the ensemble, we calculate variability for each species in the source profiles in two ways. We calculate 30 standard deviations across the replicates, r, for each day, k (i.e., within day variation) (eq 13), and 30 standard deviations across the days, k, for each replicate, r (i.e., between day variation) (eq 14).

$$\sigma_{f_{ij}}(k) = \sqrt{\frac{\sum_{r=1}^{R} (f_{ijr}(k) - \bar{f}_{ij}(k))^2}{R-1}} \quad (13)$$

$$\sigma_{f_{ij}}(r) = \sqrt{\frac{\sum_{k=1}^{K} (f_{ijk}(r) - \bar{f}_{ij}(r))^2}{K-1}} \quad (14)$$

SA for a Long-Term Data Set. Long-term SA is conducted for a 9.5 year data set (8/1/98−12/31/07) with 3107 days of measurement data collected from the Jefferson St. SEARCH site (JST) in Atlanta, GA.[28] We use a method that uses gas concentrations of SO_2, CO, and NO_x to constrain the solutions and is referred to as CMB-GC and very similar to CMB-LGO, another method that uses gas constraints.[19] We conduct SA using MBSPs, EBSPs, and BBSPs for nine source categories: gasoline vehicles (GV), diesel vehicles (DV), dust (DUST), biomass burning (BURN), coal combustion (COAL), and ammonium sulfate, ammonium bisulfate, ammonium nitrate, and other organic carbon (OC), which largely represents secondary organic carbon (SOC). We use winter EBSPs and BBSPs from November to March and summer EBSPs and BBSPs from April to October. When using BBSPs, 10 source profiles are sampled from the 900 distributions and result in 10 SAs for each day. This formulation results in a distribution of
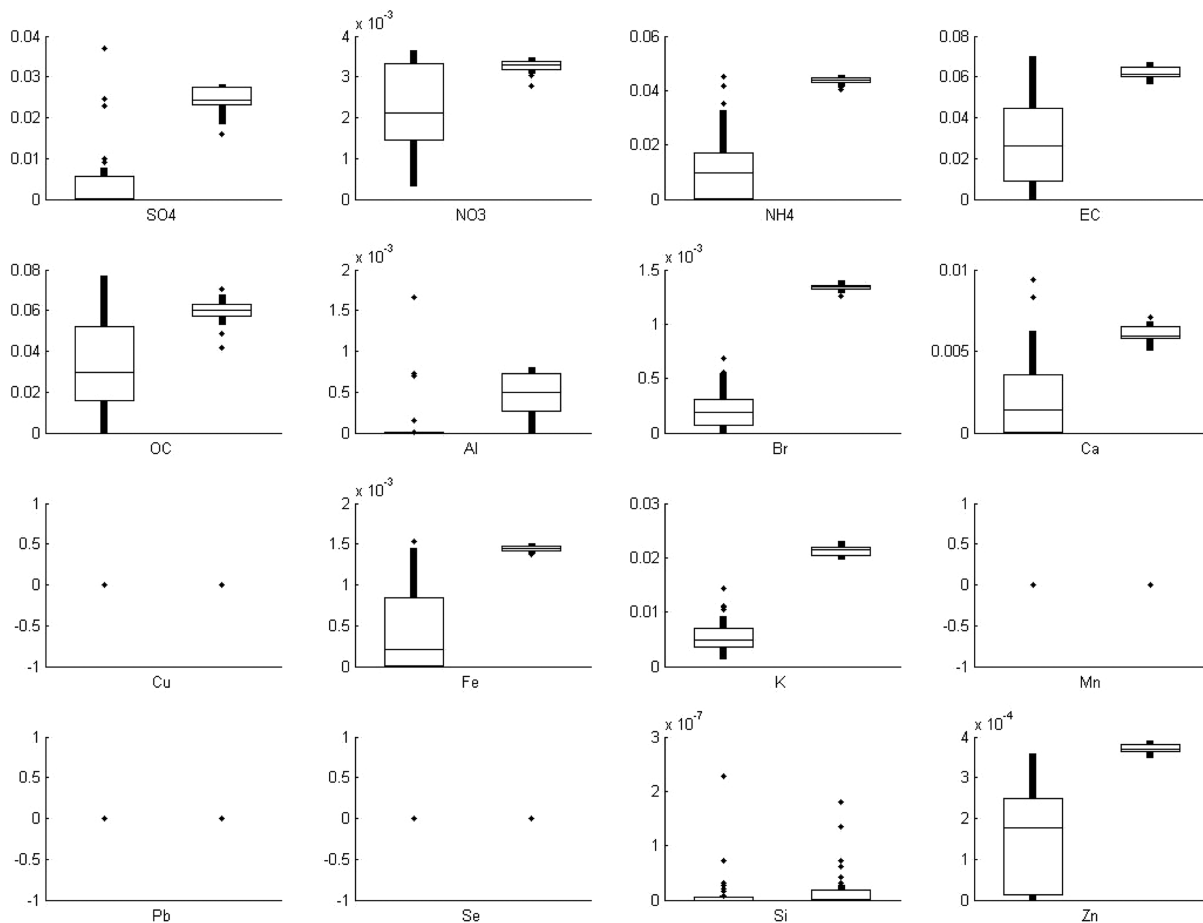
Figure 1. Boxplots of within day variation $[\sigma_{f_{ij}}(k)]$ and between day variation $[\sigma_{f_{ij}}(r)]$ for 16 species in the BURN summer Bayesian profile using non-informative priors (BBSP-NIP).

10 daily source impacts rather than a single value with an estimated uncertainty. The average and standard deviation of the 10 SA results are treated as the daily source impact and uncertainty, respectively. These are compared to EBSP- and MBSP-based source impacts and uncertainty, which are calculated using an effective variance approach.[26] We also compare results to using the CMB-RG and PMF.[21,26] The CMB-RG and PMF results were available from 1/1/99 to 12/31/04 and used in earlier ensemble studies.[9,10]

■ RESULTS AND DISCUSSION

Ensemble Averaging. We evaluate the ensemble method for each of the three steps. First, we evaluate all three cases of the ensemble-averaged source impacts (standard, Bayesian non-informative priors, and Bayesian informative priors). We expect the overall averages and uncertainties to be very similar because the mean of the IG distribution should approximately equal the RMSE; however, this may not always be the case with informative priors. All three cases of ensemble averaging result in average source impacts and overall uncertainties that are very similar, indicating that the ensemble is stable (see Table S2 of the Supporting Information).

Source Profile Variability. The distribution of species BBSPs, shown as boxplots, of $\sigma_{f_{ij}}(r)$ (between day variation) is greater than $\sigma_{f_{ij}}(k)$ (within day variation), indicating that between day variation is greater than within day variation (summer BURN profile using non-informative priors in Figure

1). In addition, the average ratio of the between day variability to within day variation, $[\sigma_{f_{ij}}(r)/\sigma_{f_{ij}}(k)]$, ranges from 1 (e.g., Pb and Zn in DUST profiles) to more than 16 (Si in summer DUST profile) (see Tables S3 and S4 of the Supporting Information). BBSPs are expected to be more variable across days than within days because ensemble-averaged source impacts used to derive source profiles have greater variability across days than within days. This indicates that variability in meteorology (e.g., because of changes in source region, atmospheric processing, and emission composition) plays a more important role in source profile variability than the uncertainty of ensemble source impacts that were used to derive the source profiles.

The new source profiles derived using Bayesian and standard ensembles are most different from MBSPs for BURN and COAL (see panels a−e of Figure S2 of the Supporting Information). BURN profiles show strong seasonality for Br, Ca, NH₄, and K, which are higher in summer profiles (see Figure S2d of the Supporting Information). This suggests that seasonal variability may be driven in part by variation in fuel type because summer impacts from biomass burning have contributions from long-range transport of western U.S. wildfires, whereas winter/early spring impacts are expected to be dominated by the local prescribed fires that occur predominately in the early spring. In addition, the summer BURN profiles are enriched in Ca, suggesting entrainment of crustal material in summer BURN emissions. Bayesian-derived
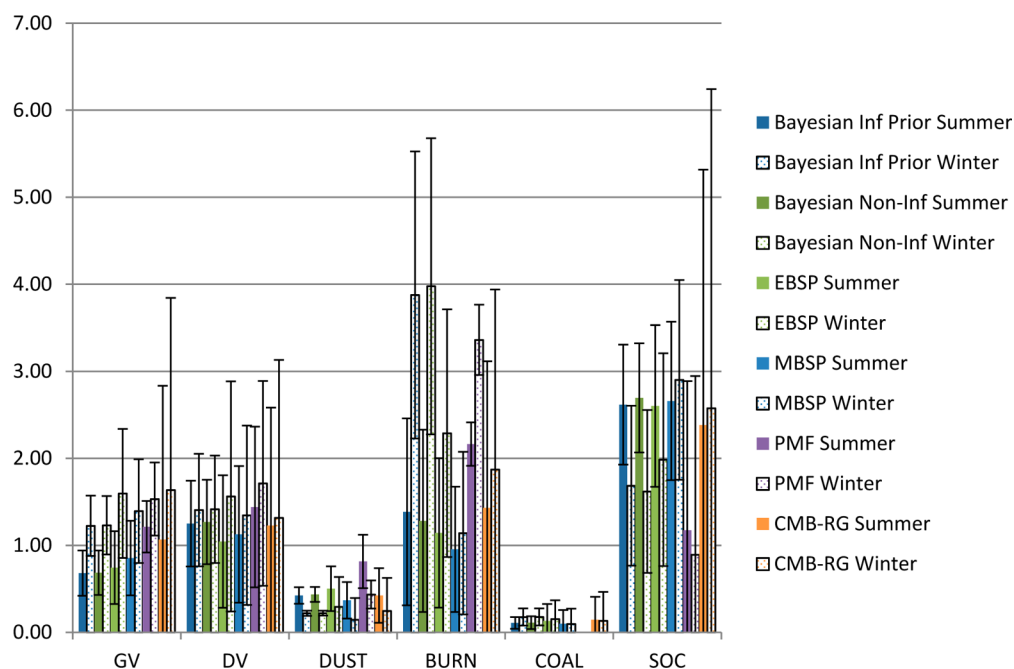
Figure 2. Average source impacts and overall uncertainties (as defined in eq 12) for primary source categories and SOC from 1999 to 2004 (results are not shown for ammonium sulfate, ammonium bisulfate, and ammonium nitrate).

COAL profiles also have differences from the MBSP profile (see Figure S2e of the Supporting Information). Most significantly, the Bayesian COAL profiles have lower OC than MBSPs. In addition, there is a distinct seasonality: higher OC in winter versus summer. This is in contrast to the EBSP COAL profiles derived by Lee et al.,[10] which have higher OC in summer than in winter, likely because of the ability of this method to include some secondary OC formation.

New GV source profiles have OC/elemental carbon (EC) ratios of ~2.2, very similar to the MBSP ratio of ~2.3. For DV, the EC/OC ratio is approximately ~4.1, slightly higher than MBSP ratios of 3.7. Some species, such as OC, have smaller variation in OC in GV than MBSPs. In addition, the OC/EC ratios in GV profiles do not show a distinct seasonality. DUST profiles are very similar to MBSPs. However, DUST profiles derived by Lee et al.[10] had ~0.2 OC, higher than in this study (~0.07), suggesting that the DUST profiles derived in this work do not reflect a mixed dust source containing traffic dust emissions.

Source profiles are also evaluated by analyzing the distributions of species in the BBSPs (see panels a–e of Figure S4 of the Supporting Information). The limits of species concentrations were set to be between $^1/_3$ and 3 times the average values in MBSPs. For some species, their values in the BBSPs are distributed between these limits; these are typically major and tracer species for a given source. However, the modes of these distributions are typically the lower limit and, occasionally, the upper allowable limit. For example, for about a third of the days, the Bayesian summer BURN profiles result in EC values of 0.003, the minimum allowable limit (see Figure S4d of the Supporting Information). This suggests that, for those days, BURN profiles may not have converged to a realistic source profile. However, because this occurs only in a minority of days and 10 of 900 source profiles are sampled for each day in the long-term SA, the effect is minimal. A consequence of this is that uncertainties of BBSPs are not necessarily lower than MBSPs. Nevertheless, for some

important tracer species, such as potassium in BURN, the distributions show distinct seasonality and variation. In the winter, the distribution of potassium is tighter and has a lower mean than in the summer (see Figure S4d of the Supporting Information).

Long-Term SA. Both ensemble methods affect the amount of mass apportioned to SOC and biomass burning by exhibiting strong seasonal differences. When using CMB-RG and CMB-GC with MBSPs, wintertime SOC levels are comparable to or slightly greater than summertime levels (Figure 2 and Table S5 of the Supporting Information). PMF also has little seasonal variation in SOC but suffers from potentially underestimating SOC in the summer. CMB-GC has a clear summer/winter split for SOC of 2.66/1.41 μg m^{-3} with BBSPs and 2.55/1.81 μg m^{-3} with EBSPs. The largest seasonal difference using BBSPs and EBSPs is for biomass burning. The summer/winter split is 1.63/3.95 μg m^{-3} with BBSPs and 1.21/2.26 μg m^{-3} with EBSPs. Having more biomass burning impacts in the winter is expected because both prescribed fires and fireplace usage are greater in these months. This seasonal variation is only slightly evident in CMB-GC with MBSPs (1.59/1.73 μg m^{-3}) and PMF (2.70/2.85 μg m^{-3}). Seasonal variation is also seen for GV using BBSPs and EBSPs, which are thought to have greater impacts in winter when cold-start emissions contribute significantly to GV emissions and when meteorological conditions lead to less dispersion.

In CMB, the reduced χ^2 value is often used as a metric for goodness of fit. Using BBSPs leads to comparable but higher reduced χ^2 values than with EBSPs or MPSPs (Table 1). Nevertheless, one important limitation of receptor models that is addressed with BBSPs is that zero-impact days are drastically reduced, a consequence of averaging 10 SA results per day. Typical of receptor models, all three predict total mass to approximately 90% of measured PM$_{2.5}$.

Source impact uncertainties using BBSPs are generally smaller than using EBSPs and MBSPs for all source categories, except biomass burning (see Figure S3 of the Supporting

Table 1. CMB-GC SA Evaluation Metrics Using Four Source Profile Sets for 8/31/98−12/31/07 (3107 Days of SA Results out of 3149 Total Days): BBSPs with Informative Priors (BBSP-IP), BBSPs with Non-informative Priors (BBSP-NIP), EBSPs, and MBSPs

	BBSP-IP	BBSP-NIP	EBSP	MBSP
reduced χ^2	5.28	5.70	3.45	4.86
predicted/observed PM mass	0.94	0.93	0.90	0.87
	zero impact days			
	informative priors	non-informative priors	EBSP	MBSP
GV	0	0	0	0
DV	3	6	204	154
DUST	0	0	15	54
BURN	0	0	4	5
COAL	9	9	184	267
SOC	24	25	60	25

Information). Because the uncertainties in BBSPs come from the standard deviation of 10 sets of SA, the higher uncertainties in biomass burning are reflective of a higher variation in BURN source profiles. This indicates that biomass burning impacts are a major source of uncertainty in SA work. In addition, the 10 sets of SA can each be used for 10 different epidemiologic analyses. This can provide a direct way to estimate uncertainties associated with the SA results in health analyses.

Evaluation of the Method. A major assumption in our method is that SA errors between each method's source impact and the ensemble average are normally distributed with a mean of 0. Three SA methods, CMB-GC with MBSPs, CMB-RG, and PMF, had results for 1994−2004, of which July 2001 and January 2002 results for CMB-GC and PMF were used in the ensemble. We compared the 1999−2004 results against the long-term SA from both Bayesian-based ensemble cases. Histograms of errors between Bayesian-based source impacts and CMB-GC with MBSPs, PMF, and CMB-RG (see Figure S4 of the Supporting Information) show that the errors can be

reasonably taken to be normally distributed, supporting eq 5, a major assumption in this work. In addition, the error histograms are not centered at 0 for winter time SOC and BURN impacts from CMB-based methods using MBSPs. This indicates the distinct bias of traditional CMB-based methods: winter time SOC is overestimated, and winter time BURN impacts are underestimated. In addition, SOC impact errors from PMF are centered at ∼1 in the summer, indicating an overall underestimation of summertime SOC from PMF (see the Supporting Information for further discussion of bias).

To further evaluate the various SA methods, we compare results for BURN and SOC impacts to independent measurements of levoglucosan, water-soluble organic carbon (WSOC), and water-soluble potassium (K^+). In 2007, a field campaign was undertaken to measure levoglucosan, a tracer for biomass burning, and WSOC, at the South Dekalb (SDK) site located approximately 10 miles southeast of JST. Given this proximity, the measurements of levoglucosan and WSOC at SDK are taken as representative of conditions of JST. There are a total of 55 samples, taken every sixth day, and we compare BURN and SOC impacts from five SA methods for the corresponding days: CMB-GC with MBSPs, EBSPs, two BBSPs (with non-informative and informative priors), and PMF. It should be noted that PMF was rerun for a data set from 1999 to 2007 that included fractionated OC data. We make three comparisons: BURN impacts with both levoglucosan and K^+ measurements and the sum of BURN and SOC impacts with WSOC (Figure 3 and Table S5 of the Supporting Information).

All five of the SA methods apportion the sum of BURN and SOC impacts similarly, and all methods have similar correlations. The highest correlations are for CMB-GC−MBSP and PMF ($R^2 \sim 0.7$) and the lowest correlations are for CMB-GC−BBSP using informative priors ($R^2 \sim 0.6$) (Figure 3). However, the methods split the WSOC into BURN and SOC fractions differently. The BBSPs have the highest correlation ($R^2 \sim 0.5−0.6$) between BURN impacts and levoglucosan, while the other methods have $R^2 \sim 0.02−0.3$.
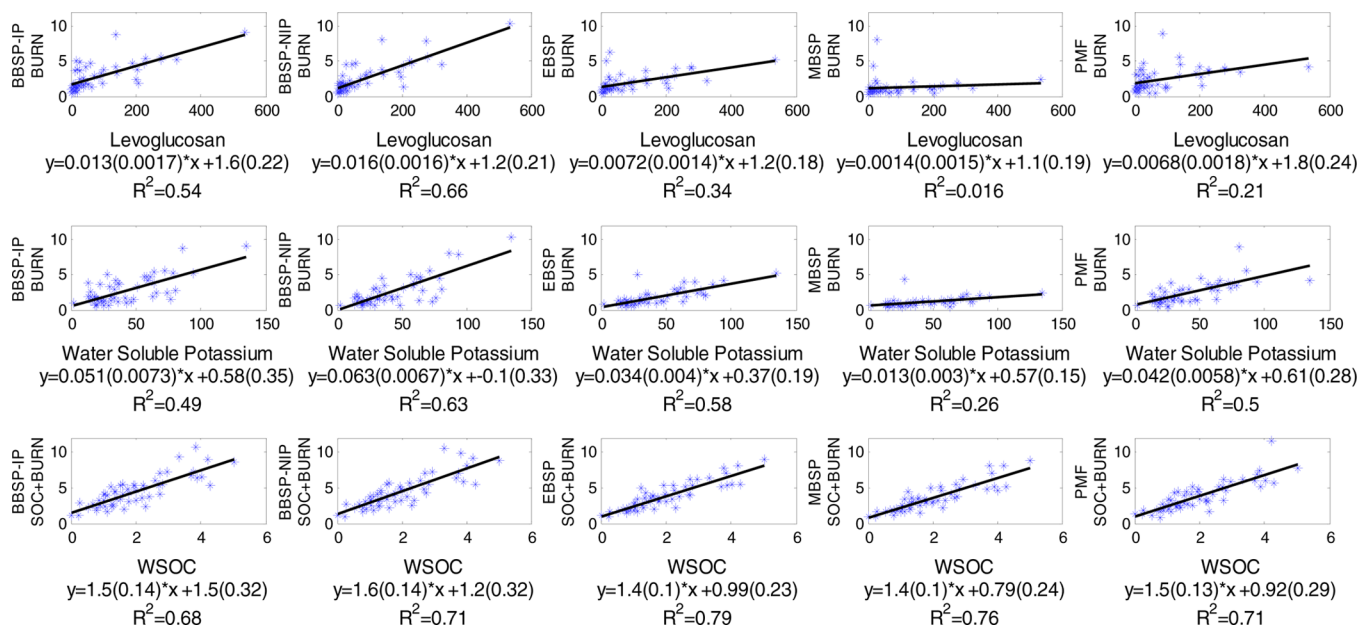

Figure 3. Comparison of source impacts for BURN and SOC and WSOC, levoglucosan, and K^+. The first row compares BURN and levoglucosan. The second row compares BURN and K^+. The last row compares the sum of SOC and BURN impacts and WSOC.

The BBSPs also have the highest correlation ($R^2 \sim 0.5-0.6$) between BURN impacts and K^+.

WSOC is viewed as having two major sources: biomass burning and secondary organic aerosol (SOA) formation.[29,30] The Bayesian approach produces a higher correlation between biomass burning and both levoglucosan and water-soluble potassium than the other methods, suggesting a more accurate split between biomass burning and SOC. Using non-informative priors produces a higher correlation with levoglucosan than using informative priors and may be due to the influence of CMAQ. There is a greater influence from CMAQ when using non-informative priors because all SA methods are essentially treated equally. CMAQ is weighted less when using informative priors. Because there is no accepted method for calculating uncertainties in CMAQ, we still use non-informative priors for CMAQ, while the other SA methods use informative priors. This further suggests that uncertainties calculated by the routine-specific approaches are not appropriate in comparing the accuracy of the different SA methods.

One limitation of the ensemble-averaging method is that it is dependent upon short-term applications of CMAQ (and CMB-MM, but it expected that CTMs will be used more than CMB-MM in ensemble averaging). As more CTM-based SA is conducted, the Bayesian method should be applied using short-term applications for different time periods. The use of informative priors led to lower correlations between BURN impacts and measured levoglucosan than with non-informative priors. However, SA results using non-informative priors are, in general, highly correlated with informative priors. In this work, we use IG priors with a normal likelihood function, in part, because the resulting posterior distributions have closed-form expressions that can be sampled from efficiently. The use of non-conjugate priors may lead to improved results.

■ ASSOCIATED CONTENT

Ⓢ Supporting Information

Tables S1–S8 and Figures S1–S6. This material is available free of charge via the Internet at http://pubs.acs.org.

■ AUTHOR INFORMATION

Corresponding Author

*Telephone: 206-250-6480. Fax: 404-894-8266. E-mail: siv@gatech.edu.

Notes

The authors declare no competing financial interest.

■ REFERENCES

(1) Lim, S. S.; Vos, T.; Flaxman, A. D.; Danaei, G.; Shibuya, K.; Adair-Rohani, H.; Amann, M.; Anderson, H. R.; Andrews, K. G.; Aryee, M.; Atkinson, C.; Bacchus, L. J.; Bahalim, A. N.; Balakrishnan, K.; Balmes, J.; Barker-Collo, S.; Baxter, A.; Bell, M. L.; Blore, J. D.; Blyth, F.; Bonner, C.; Borges, G.; Bourne, R.; Boussinesq, M.; Brauer, M.; Brooks, P.; Bruce, N. G.; Brunekreef, B.; Bryan-Hancock, C.; Bucello, C.; Buchbinder, R.; Bull, F.; Burnett, R. T.; Byers, T. E.; Calabria, B.; Carapetis, J.; Carnahan, E.; Chafe, Z.; Charlson, F.; Chen, H.; Chen, J. S.; Cheng, A. T.-A.; Child, J. C.; Cohen, A.; Colson, K. E.; Cowie, B. C.; Darby, S.; Darling, S.; Davis, A.; Degenhardt, L.; Dentener, F.; Des Jarlais, D. C.; Devries, K.; Dherani, M.; Ding, E. L.; Dorsey, E. R.; Driscoll, T.; Edmond, K.; Ali, S. E.; Engell, R. E.; Erwin, P. J.; Fahimi, S.; Falder, G.; Farzadfar, F.; Ferrari, A.; Finucane, M. M.; Flaxman, S.; Fowkes, F. G. R.; Freedman, G.; Freeman, M. K.; Gakidou, E.; Ghosh, S.; Giovannucci, E.; Gmel, G.; Graham, K.; Grainger, R.; Grant, B.; Gunnell, D.; Gutierrez, H. R.; Hall, W.; Hoek, H. W.; Hogan, A.; Hosgood, H. D., III; Hoy, D.; Hu, H.; Hubbell, B. J.; Hutchings, S. J.; Ibeanusi, S. E.; Jacklyn, G. L.; Jasrasaria, R.; Jonas, J. B.; Kan, H.; Kanis, J. A.; Kassebaum, N.; Kawakami, N.; Khang, Y.-H.; Khatibzadeh, S.; Khoo, J.-P.; Kok, C.; Laden, F.; Lalloo, R.; Lan, Q.; Lathlean, T.; Leasher, J. L.; Leigh, J.; Li, Y.; Lin, J. K.; Lipshultz, S. E.; London, S.; Lozano, R.; Lu, Y.; Mak, J.; Malekzadeh, R.; Mallinger, L.; Marcenes, W.; March, L.; Marks, R.; Martin, R.; McGale, P.; McGrath, J.; Mehta, S.; Mensah, G. A.; Merriman, T. R.; Micha, R.; Michaud, C.; Mishra, V.; Hanafiah, K. M.; Mokdad, A. A.; Morawska, L.; Mozaffarian, D.; Murphy, T.; Naghavi, M.; Neal, B.; Nelson, P. K.; Nolla, J. M.; Norman, R.; Olives, C.; Omer, S. B.; Orchard, J.; Osborne, R.; Ostro, B.; Page, A.; Pandey, K. D.; Parry, C. D. H.; Passmore, E.; Patra, J.; Pearce, N.; Pelizzari, P. M.; Petzold, M.; Phillips, M. R.; Pope, D.; Pope, C. A., III; Powles, J.; Rao, M.; Razavi, H.; Rehfuess, E. A.; Rehm, J. T.; Ritz, B.; Rivara, F. P.; Roberts, T.; Robinson, C.; Rodriguez-Portales, J. A.; Romieu, I.; Room, R.; Rosenfeld, L. C.; Roy, A.; Rushton, L.; Salomon, J. A.; Sampson, U.; Sanchez-Riera, L.; Sanman, E.; Sapkota, A.; Seedat, S.; Shi, P.; Shield, K.; Shivakoti, R.; Singh, G. M.; Sleet, D. A.; Smith, E.; Smith, K. R.; Stapelberg, N. J. C.; Steenland, K.; Stöckl, H.; Stovner, L. J.; Straif, K.; Straney, L.; Thurston, G. D.; Tran, J. H.; Van Dingenen, R.; van Donkelaar, A.; Veerman, J. L.; Vijayakumar, L.; Weintraub, R.; Weissman, M. M.; White, R. A.; Whiteford, H.; Wiersma, S. T.; Wilkinson, J. D.; Williams, H. C.; Williams, W.; Wilson, N.; Woolf, A. D.; Yip, P.; Zielinski, J. M.; Lopez, A. D.; Murray, C. J. L.; Ezzati, M. A comparative risk assessment of burden of disease and injury attributable to 67 risk factors and risk factor clusters in 21 regions, 1990−2010: A systematic analysis for the Global Burden of Disease Study 2010. *Lancet* **2012**, *380* (9859), 2224−2260.

(2) Dockery, D. W.; Pope, C. A.; Xu, X. P.; Spengler, J. D.; Ware, J. H.; Fay, M. E.; Ferris, B. G.; Speizer, F. E. An association between air-pollution and mortality in 6 United States cities. *N. Engl. J. Med.* **1993**, *329* (24), 1753−1759.

(3) Laden, F.; Neas, L. M.; Dockery, D. W.; Schwartz, J. Association of fine particulate matter from different sources with daily mortality in six US cities. *Environ. Health Perspect.* **2000**, *108* (10), 941−947.

(4) Hopke, P. K.; Ito, K.; Mar, T.; Christensen, W. F.; Eatough, D. J.; Henry, R. C.; Kim, E.; Laden, F.; Lall, R.; Larson, T. V.; Liu, H.; Neas, L.; Pinto, J.; Stolzel, M.; Suh, H.; Paatero, P.; Thurston, G. D. PM source apportionment and health effects: 1. Intercomparison of source apportionment results. *J. Exposure Sci. Environ. Epidemiol.* **2006**, *16* (3), 275−286.

(5) Ito, K.; Christensen, W. F.; Eatough, D. J.; Henry, R. C.; Kim, E.; Laden, F.; Lall, R.; Larson, T. V.; Neas, L.; Hopke, P. K.; Thurston, G. D. PM source apportionment and health effects: 2. An investigation of intermethod variability in associations between source-apportioned fine particle mass and daily mortality in Washington, DC. *J. Exposure Sci. Environ. Epidemiol.* **2006**, *16* (4), 300−310.

(6) Mar, T. F.; Ito, K.; Koenig, J. Q.; Larson, T. V.; Eatough, D. J.; Henry, R. C.; Kim, E.; Laden, F.; Lall, R.; Neas, L.; Stolzel, M.; Paatero, P.; Hopke, P. K.; Thurston, G. D. PM source apportionment and health effects. 3. Investigation of inter-method variations in associations between estimated source contributions of PM$_{2.5}$ and daily mortality in Phoenix, AZ. *J. Exposure Sci. Environ. Epidemiol.* **2006**, *16* (4), 311−320.

(7) Sarnat, J. A.; Marmur, A.; Klein, M.; Kim, E.; Russell, A. G.; Sarnat, S. E.; Mulholland, J. A.; Hopke, P. K.; Tolbert, P. E. Fine particle sources and cardiorespiratory morbidity: An application of chemical mass balance and factor analytical source-apportionment methods. *Environ. Health Perspect.* **2008**, *116* (4), 459−466.

(8) Thurston, G. D.; Ito, K.; Mar, T.; Christensen, W. F.; Eatough, D. J.; Henry, R. C.; Kim, E.; Laden, F.; Lall, R.; Larson, T. V.; Liu, H.; Neas, L.; Pinto, J.; Stolzel, M.; Suh, H.; Hopke, P. K. Workgroup report: Workshop on source apportionment of particulate matter health effects—Intercomparison of results and implications. *Environ. Health Perspect.* **2005**, *113* (12), 1768−1774.

(9) Balachandran, S.; Pachon, J. E.; Hu, Y.; Lee, D.; Mulholland, J. A.; Russell, A. G. Ensemble-trained source apportionment of fine particulate matter and method uncertainty analysis. *Atmos. Environ.* **2012**, *61*, 387−394.

(10) Lee, D.; Balachandran, S.; Pachon, J.; Shankaran, R.; Lee, S.; Mulholland, J. A.; Russell, A. G. Ensemble-trained $PM_{2.5}$ source apportionment approach for health studies. *Environ. Sci. Technol.* **2009**, *43* (18), 7023−7031.

(11) Maier, M. L.; Balachandran, S.; Sarnat, S. E.; Turner, J. R.; Mulholland, J. A.; Russell, A. G. Application of an ensemble-trained source apportionment approach at a site impacted by multiple point sources. *Environ. Sci. Technol.* **2013**, *47* (8), 3743−3751.

(12) Kashiwagi, N. Chemical mass balance when an unknown source exists. *Environmetrics* **2004**, *15* (8), 777−796.

(13) Keats, A.; Cheng, M. T.; Yee, E.; Lien, F. S. Bayesian treatment of a chemical mass balance receptor model with multiplicative error structure. *Atmos. Environ.* **2009**, *43* (3), 510−519.

(14) Lingwall, J. W.; Christensen, W. F. Pollution source apportionment using a priori information and positive matrix factorization. *Chemom. Intell. Lab. Syst.* **2007**, *87* (2), 281−294.

(15) Lingwall, J. W.; Christensen, W. F.; Reese, C. S. Dirichlet based Bayesian multivariate receptor modeling. *Environmetrics* **2008**, *19* (6), 618−629.

(16) Park, E. S.; Guttorp, P.; Henry, R. C. Multivariate receptor modeling for temporally correlated data by using MCMC. *J. Am. Stat. Assoc.* **2001**, *96* (456), 1171−1183.

(17) Park, E. S.; Oh, M. S.; Guttorp, P. Multivariate receptor models and model uncertainty. *Chemom. Intell. Lab. Syst.* **2002**, *60* (1−2), 49−67.

(18) Park, E. S.; Spiegelman, C. H.; Henry, R. C. Bilinear estimation of pollution source profiles and amounts by using multivariate receptor models. *Environmetrics* **2002**, *13* (7), 775−798.

(19) Marmur, A.; Unal, A.; Mulholland, J. A.; Russell, A. G. Optimization-based source apportionment of $PM_{2.5}$ incorporating gas-to-particle ratios. *Environ. Sci. Technol.* **2005**, *39* (9), 3245−3254.

(20) Zheng, M.; Cass, G. R.; Schauer, J. J.; Edgerton, E. S. Source apportionment of $PM_{2.5}$ in the southeastern United States using solvent-extractable organic compounds as tracers. *Environ. Sci. Technol.* **2002**, *36* (11), 2361−2371.

(21) Paatero, P.; Tapper, U. Positive matrix factorization—A nonnegative factor model with optimal utilization of error-estimates of data values. *Environmetrics* **1994**, *5* (2), 111−126.

(22) Byun, D.; Schere, K. L. Review of the governing equations, computational algorithms, and other components of the Models-3 Community Multiscale Air Quality (CMAQ) modeling system. *Appl. Mech. Rev.* **2006**, *59* (1−6), 51−77.

(23) Zheng, M.; Cass, G. R.; Ke, L.; Wang, F.; Schauer, J. J.; Edgerton, E. S.; Russell, A. G. Source apportionment of daily fine particulate matter at Jefferson street, Atlanta, GA, during summer and winter. *J. Air Waste Manage. Assoc.* **2007**, *57* (2), 228−242.

(24) Baek, J. Improving aerosol simulations: Assessing and improving emissions and secondary organic aerosol formation in air quality modeling. Ph.D. Dissertation, Georgia Institute of Technology, Atlanta, GA, 2009.

(25) United States Environmental Protection Agency (U.S. EPA). *EPA-CMB8.2 User's Manual*; Office of Air Quality and Standards, U.S. EPA: Research Triangle Park, NC, 2004; EPA-452/R-04-011.

(26) Watson, J. G.; Cooper, J. A.; Huntzicker, J. J. The effective variance weighting for least-squares calculations applied to the mass balance receptor model. *Atmos. Environ.* **1984**, *18* (7), 1347−1355.

(27) Pachon, J. E.; Balachandran, S.; Hu, Y. T.; Weber, R. J.; Mulholland, J. A.; Russell, A. G. Comparison of SOC estimates and uncertainties from aerosol chemical composition and gas phase data in Atlanta. *Atmos. Environ.* **2010**, *44* (32), 3907−3914.

(28) Hansen, D. A.; Edgerton, E. S.; Hartsell, B. E.; Jansen, J. J.; Kandasamy, N.; Hidy, G. M.; Blanchard, C. L. The southeastern aerosol research and characterization study: Part 1—Overview. *J. Air Waste Manage. Assoc.* **2003**, *53* (12), 1460−1471.

(29) Sullivan, A. P.; Weber, R. J. Chemical characterization of the ambient organic aerosol soluble in water: 2. Isolation of acid, neutral, and basic fractions by modified size-exclusion chromatography. *J. Geophys. Res.: Atmos.* **2006**, *111* (D5), D05314.

(30) Weber, R. J.; Sullivan, A. P.; Peltier, R. E.; Russell, A.; Yan, B.; Zheng, M.; de Gouw, J.; Warneke, C.; Brock, C.; Holloway, J. S; Atlas, E. L.; Edgerton, E. A study of secondary organic aerosol formation in the anthropogenic-influenced southeastern United States. *J. Geophys. Res.: Atmos.* **2007**, *112* (D13), D13302.